Cell adhesion geometry regulates non-random DNA segregation and asymmetric cell fates in mouse skeletal muscle stem cells.

Siham Yennek, Mithila Burute, Manuel Théry, Shahragim Tajbakhsh

Cell Reports
Report

Cell Adhesion Geometry Regulates Non-Random DNA Segregation and Asymmetric Cell Fates in Mouse Skeletal Muscle Stem Cells

Siham Yennek,[1,2] Mithila Burute,[3,4,5] Manuel Théry,[3,5] and Shahragim Tajbakhsh[1,*]
[1]Institut Pasteur, Stem Cells & Development, Department of Developmental & Stem Cell Biology, CNRS URA 2578, 25 rue du Dr. Roux, Paris F-75015, France
[2]Sorbonne Universités, UPMC, University of Paris 06, IFD-ED 515, 4 Place Jussieu, Paris 75252, France
[3]Institut de Recherche en Technologie et Science pour le Vivant, UMR5168, CEA/UJF/INRA/CNRS, 17 rue des Martyrs, Grenoble 38054, France
[4]CYTOO SA, 7 Parvis Louis Néel, BP50, Grenoble 38040, France
[5]Hôpital Saint Louis, Institut Universitaire d'Hematologie, U1160, INSERM/AP-HP/Université Paris Diderot, 1 Avenue Claude Vellefaux, Paris 75010, France
*Correspondence: shahragim.tajbakhsh@pasteur.fr
http://dx.doi.org/10.1016/j.celrep.2014.04.016

SUMMARY

Cells of several metazoan species have been shown to non-randomly segregate their DNA such that older template DNA strands segregate to one daughter cell. The mechanisms that regulate this asymmetry remain undefined. Determinants of cell fate are polarized during mitosis and partitioned asymmetrically as the spindle pole orients during cell division. Chromatids align along the pole axis; therefore, it is unclear whether extrinsic cues that determine spindle pole position also promote non-random DNA segregation. To mimic the asymmetric divisions seen in the mouse skeletal stem cell niche, we used micropatterns coated with extracellular matrix in asymmetric and symmetric motifs. We show that the frequency of non-random DNA segregation and transcription factor asymmetry correlates with the shape of the motif and that these events can be uncoupled. Furthermore, regulation of DNA segregation by cell adhesion occurs within a defined time interval. Thus, cell adhesion cues have a major impact on determining both DNA segregation patterns and cell fates.

INTRODUCTION

Stem cells can exhibit distinct behaviors in different physiological contexts, such as organogenesis and regeneration. For example, some cells can divide asymmetrically by partitioning a variety of subcellular components, whereas others can divide symmetrically. These types of divisions can be governed by extrinsic stimuli that relay to intrinsic regulators to generate invariant, or randomized, cell divisions consecutively (Yennek and Tajbakhsh, 2013). Numerous intrinsic cell fate regulators have been identified in organisms ranging from flies to humans (Li, 2013; Neumüller and Knoblich, 2009). Of these, perhaps the most intriguing is the asymmetric segregation of old and new template DNA strands, referred to as non-random DNA segregation (or template DNA strand segregation, biased DNA segregation, or "immortal" DNA; Tajbakhsh and Gonzalez, 2009; Yennek and Tajbakhsh, 2013).

Semiconservative replication of DNA results in chromatids containing older template and nascent DNA strands. Label-retaining experiments with nucleotide analogs suggested that labeled DNA strands can persist in certain conditions after extensive cell divisions (Yennek and Tajbakhsh, 2013). These observations led to the hypothesis that chromatids containing older DNA strands segregate collectively to only one of the daughter cells in consecutive asymmetric divisions (Cairns, 1975); however, unequivocal evidence for long-term "immortality" of old DNA strands in vivo is lacking. Support for non-random DNA segregation comes from studies in several tissues, including skeletal muscle (Elabd et al., 2013; Falconer et al., 2010; Karpowicz et al., 2005; Potten et al., 2002; Quyn et al., 2010; Rocheteau et al., 2012; Shinin et al., 2006; Yadlapalli and Yamashita, 2013; Yennek and Tajbakhsh, 2013). Adult skeletal muscle stem cells are quiescent during homeostasis and express the upstream transcription factor Pax7 (Seale et al., 2000). After muscle injury, they enter the cell cycle and generate myoblasts that will divide and differentiate, while a subpopulation of myogenic cells that retain *Pax7* expression will self-renew. During muscle regeneration, DNA and other molecules are partitioned asymmetrically or symmetrically as myogenic cells undergo mitosis (Kuang et al., 2007; Le Grand et al., 2009; Liu et al., 2012; Rocheteau et al., 2012; Shinin et al., 2006; Troy et al., 2012). Non-random DNA segregation occurs in a subpopulation of muscle stem cells, and a correlation with the fates of the resulting daughter cells has been noted (Conboy et al., 2007; Rocheteau et al., 2012; Shinin et al., 2006; Yennek and Tajbakhsh, 2013). Studies examining the mechanisms that regulate this process have focused essentially on intrinsic regulators,

notably, epigenetic marks on the DNA molecules or associated proteins postreplication (Elabd et al., 2013; Evano and Tajbakhsh, 2013; Lansdorp, 2007; Lew et al., 2008; Tajbakhsh and Gonzalez, 2009). However, cell contact, cell density, and microenvironment have also been reported to play a role in non-random DNA segregation (Freida et al., 2013; Pine et al., 2010; Shinin et al., 2006). A network of extracellular matrix (ECM) that surrounds the cell is connected to intracellular cytoskeletal actin via transmembrane proteins. Previous studies using micropatterns coated with ECM showed that its spatial distribution plays a critical role in determining the orientation of the axis of division by controlling the localization of actin-associated cues at the membrane that can interact with spindle microtubules (Minc and Piel, 2012; Théry et al., 2007). Moreover, asymmetric distribution of adhesion cues was shown to induce asymmetric spindle orientation (Théry et al., 2007), suggesting that it could further impact division symmetry by regulating non-random DNA segregation and unequal cell fate. Here, we manipulated the shape of ECM-coated micropatterns and consequently the spatial distribution of cell adhesion, and examined the fate outcome of single mouse skeletal muscle stem cells during cell division.

RESULTS

Polarized Cell Architecture Correlates with Extrinsic Adhesion Asymmetry on Micropatterns

In a previous study (Rocheteau et al., 2012), we showed that a subpopulation of skeletal muscle stem cells isolated from *Tg:Pax7-nGFP* mice can perform non-random DNA segregation (Figure S1A). This phenotype was correlated in part with the distribution of the transcription factors Pax7 (stem/progenitor) and Myogenin (differentiated). In that study, the overall frequency of asymmetry in the total population was not determined.

To investigate cell division outcomes in a controlled microenvironment, we examined single skeletal muscle stem cell divisions on fibronectin/fibrinogen-Alexa Fluor 594-coated micropatterns as described previously for other cell types (Azioune et al., 2010; Théry et al., 2005, 2007), where the differential adhesion and shape of the micropatterns were asymmetric or symmetric in design. Muscle stem cells isolated by fluorescence-activated cell sorting (FACS) using *Tg:Pax7-nGFP* mice (Figure S1B), as well as their progeny cells, are smaller in size than most somatic cells (Figure 1A), with an average surface area in culture of about 250–300 μm^2. This value was determined in an initial series of experiments when micropatterns of various sizes and shapes were designed. The micropattern size was chosen so that all cells could spread on the entire micropattern adhesive area (Azioune et al., 2010). One symmetric and two asymmetric motifs were fabricated for these studies (Figures 1B and 1C). Stainings for F-actin and alpha-tubulin showed dramatic differences in the polarity of the cells seeded on micropatterns. Actin stress fibers were prominently polarized on asymmetric micropatterns but were relatively homogeneous on the symmetric motifs, although in both cases, stainings showed high levels of cortical actin localized at the cell membrane, likely due to the constraints imposed by the micropatterns compared with a nonpatterned surface. Tubulin staining was also strikingly polarized, and to a greater extent on asymmetric motifs (Figure 1B). The polarized nature of the cells on the micropattern motifs that were made for this study is in agreement with previous observations that adhesion cues can impact cell polarity (Freida et al., 2013; Théry et al., 2005), validating the use of micropattern designs for investigating the role of adhesion cues on asymmetric cell divisions in muscle stem cells.

Non-Random DNA Segregation in Muscle Stem Cells Is Promoted on Asymmetric Micropatterns

Incorporation of nucleotide analogs into either template or nascent DNA strands can be achieved by using different labeling regimes (Figure S1A). To investigate the influence of adhesion cues on asymmetric cell divisions, in a first series of experiments we used our previously defined pulse-chase protocol to label dividing myogenic cells in vivo with 5-ethynyl-2′-deoxyuridine (EdU) from 3 to 5 days postinjury (DPI). Following one cell division of chase in vivo, the total Pax7-nGFP$^+$ myogenic population was isolated by FACS and plated on the micropatterns to allow the second division. Using this labeling regime (inclusion protocol; Figures 2A and S1A), template DNA strands were EdU positive, whereas EdU-negative cells contained nascent DNA strands after the two cell divisions of chase (Figures 2A and S1A; Rocheteau et al., 2012; Yennek and Tajbakhsh, 2013). The vast majority of micropatterns contained a single cell following plating (data not shown; see Movies S1 and S2). After a second division during the chase period, DNA segregation and cell fate outcomes were assessed by immunostaining. In some cases, videomicroscopy was used in parallel to ensure that single cells were seeded and daughter cell pairs were obtained on the patterns (Movies S1 and S2). These videos showed the extensive motility of the myogenic cells on the micropattern motifs before and after mitosis. As a control, Pax7-nGFP$^+$ myogenic cells were seeded on fibronectin/fibrinogen-Alexa Fluor 594-coated slides to assess the frequency of asymmetric divisions on a nonpatterned surface.

Strikingly, on both types of asymmetric micropattern motifs, the majority of the cells performed non-random DNA segregation with a frequency of 60%–62% (n = 2 mice; Asym1, n = 163 daughter cell pairs; Asym2, n = 189 daughter cell pairs; Figures 2B and 2C), which is significantly greater than previous results obtained at 5 DPI (Rocheteau et al., 2012). Interestingly, the frequency of non-random DNA segregation on a symmetric pattern was also relatively high at 26% (n = 2 mice; n = 106 daughter cell pairs; Figures 2B and 2C). To verify this effect of cell adhesion on DNA segregation patterns and to rule out biases due to the labeling regime, we incorporated nucleotide analogs into nascent DNA strands instead (exclusion protocol; Figure 2D). We obtained similar results, in that about 71% of cells performed non-random DNA segregation on the asymmetric patterns (n = 9 mice; Asym1, n = 328 daughter cell pairs; Asym2, n = 304 daughter cell pairs) compared with about 29% for the symmetric micropattern (n = 9 mice; n = 330 daughter cell pairs; Figures 2E and 2F). As a control, the frequency of non-random DNA segregation on a nonpatterned surface coated with fibronectin/fibrinogen-Alexa Fluor 594 was noted to be 33% (n = 5 mice; n = 76 of 231 daughter cell pairs; Figure S1C), which was not significantly higher than the frequency on the symmetric

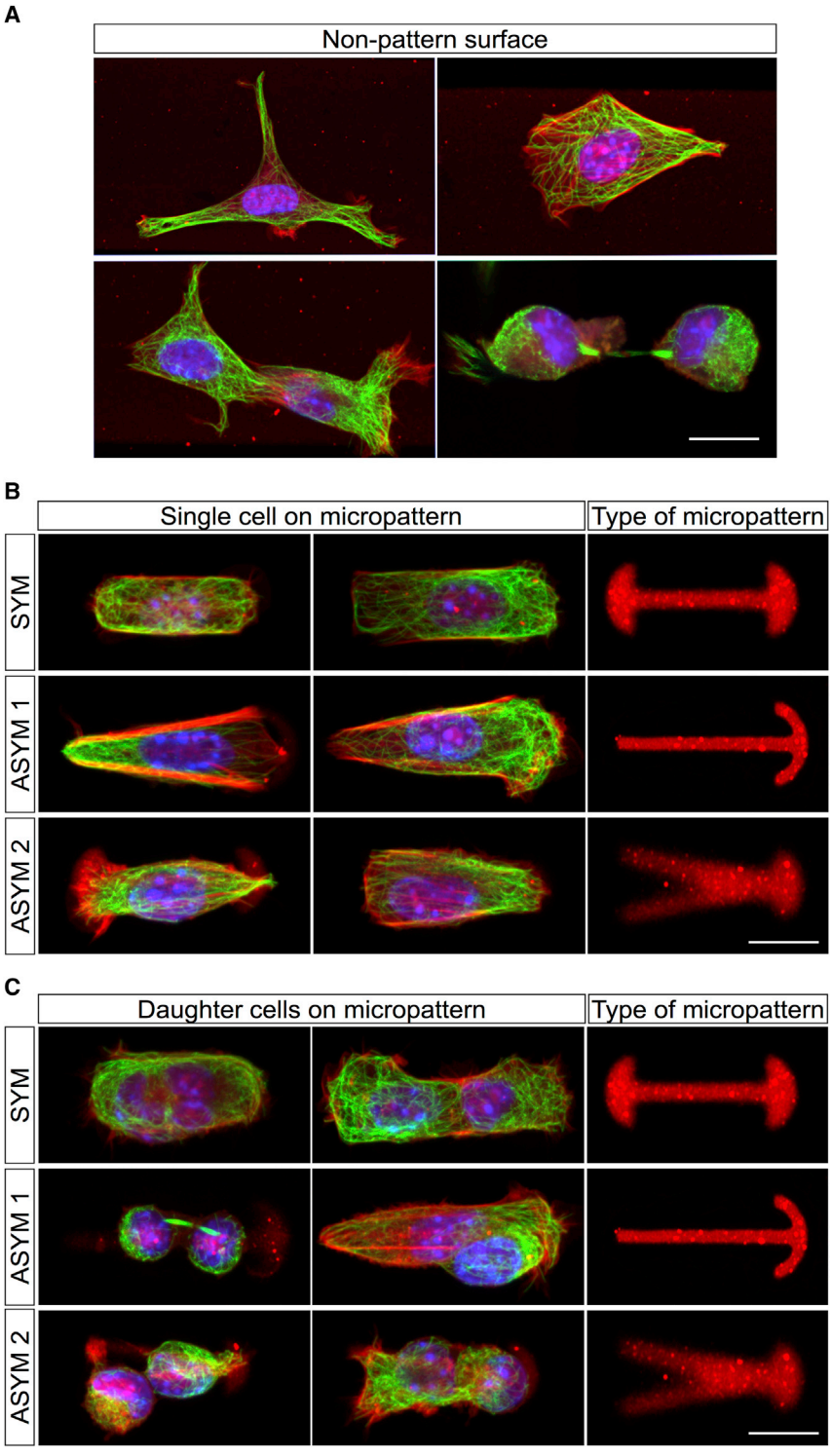

Figure 1. Muscle Stem Cells Are Polarized on Asymmetric Micropatterns

(A) Examples of muscle stem cells isolated by FACS from the TA muscle of *Tg:Pax7-nGFP* mice at 5 DPI, plated on slides coated with fibronectin/fibrinogen-Alexa Fluor 594, and then stained for actin (red) and tubulin (green).

(B) Examples of muscle stem cells isolated and treated as in (A), seeded on symmetric (top) and asymmetric (bottom two rows) micropattern motifs (two examples shown for each). Note the prominent actin stress fibers, particularly on asymmetric motifs, and in some cases the polarized distribution of tubulin on asymmetric motifs.

(C) Examples of muscle stem cells isolated and treated as in (A), seeded on symmetric (top) and asymmetric (bottom two rows) micropattern motifs (two examples shown for each). Cells were allowed to divide on the micropattern. Note that both daughter cells occupy the micropattern surface, and in some cases display polarized tubulin on the asymmetric motifs.

Scale bars: (A), 10 μm; (B and C), 20 μm.

micropattern ($p > 0.37$). In this experiment, we used cytochalasin D to block cell separation after mitosis to ensure the identification of daughter cell pairs, as this drug does not appear to overtly interfere with non-random DNA segregation when applied for a short interval (Conboy et al., 2007; Huh and Sherley, 2011; Karpowicz et al., 2005; S.Y. and S.T., unpublished data). As an additional control for cell division ex vivo, in some experiments we added a second nucleotide analog to the cells on micropatterns prior to cell division to ensure correct nucleotide uptake by both daughter cells during the experiment (Figure S1D). We performed the remaining experiments in this study using the exclusion protocol because it exposes cells for a shorter period to the nucleotide analogs.

Asymmetric Daughter Cell Fates in Muscle Stem Cells Are Promoted on Asymmetric Micropatterns

We next asked whether manipulating the cell adhesion topology would alter the outcome of the resulting daughter cell fates. We showed previously that old DNA strands segregated to the stem cell and that asymmetric cell fates, as assessed by the differential distribution of the transcription factors Pax7 and Myogenin after mitosis, were correlated in part with non-random DNA segregation (Rocheteau et al., 2012). The link between these distinct asymmetric readouts has not yet been established. To assess the effect of adhesion cues on these asymmetries, we analyzed DNA and transcription factor segregation patterns by staining for EdU, Pax7, and Myogenin. When we examined the total Pax7-nGFP$^+$ population on the symmetric motif, we found that the majority of the cells performed random DNA segregation (70%; n = 78 of

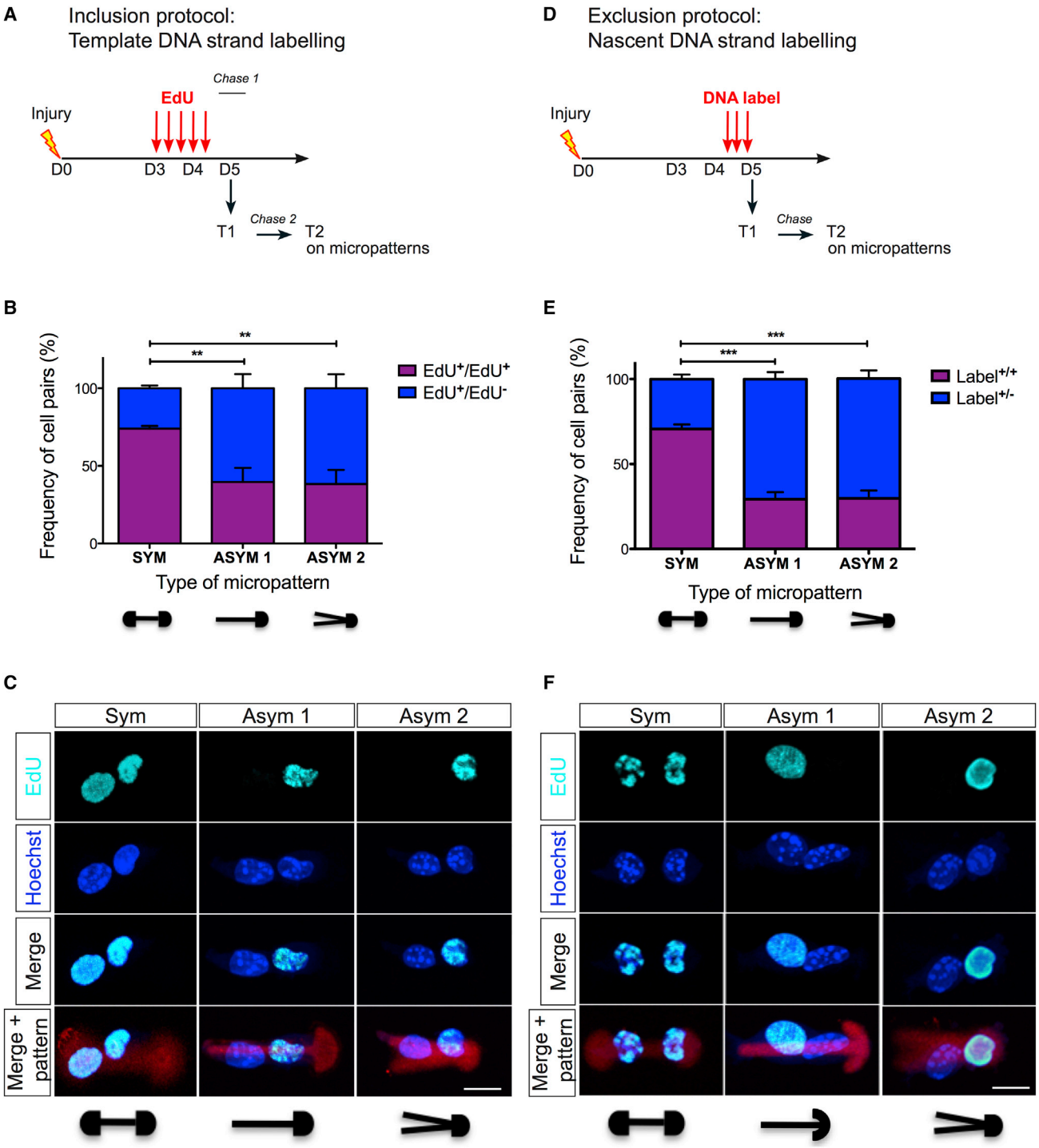

Figure 2. Extrinsic Cues Mediated by Cell Adhesion Regulate the Frequency of Non-Random DNA Segregation on Micropatterns

(A) Scheme illustrating labeling of old template DNA strands. To label older template DNA strands ("inclusion" protocol), label was added for several rounds of cell division to label both DNA strands. After two cell divisions, non-random DNA segregation patterns were assessed empirically.

(B) Histogram showing the frequencies of non-random DNA segregation on one symmetric and two asymmetric micropatterns. Pax7-nGFP$^+$ myogenic cells were isolated by FACS from TA muscle of *Tg:Pax7-nGFP* mice as indicated in (A) ($p < 0.007$). Error bars indicated as SEM.

(C) Click-iT detection of EdU in examples of daughter cell pairs indicated in (B) after two divisions during the chase period. The micropattern shapes are in red (scheme below).

(legend continued on next page)

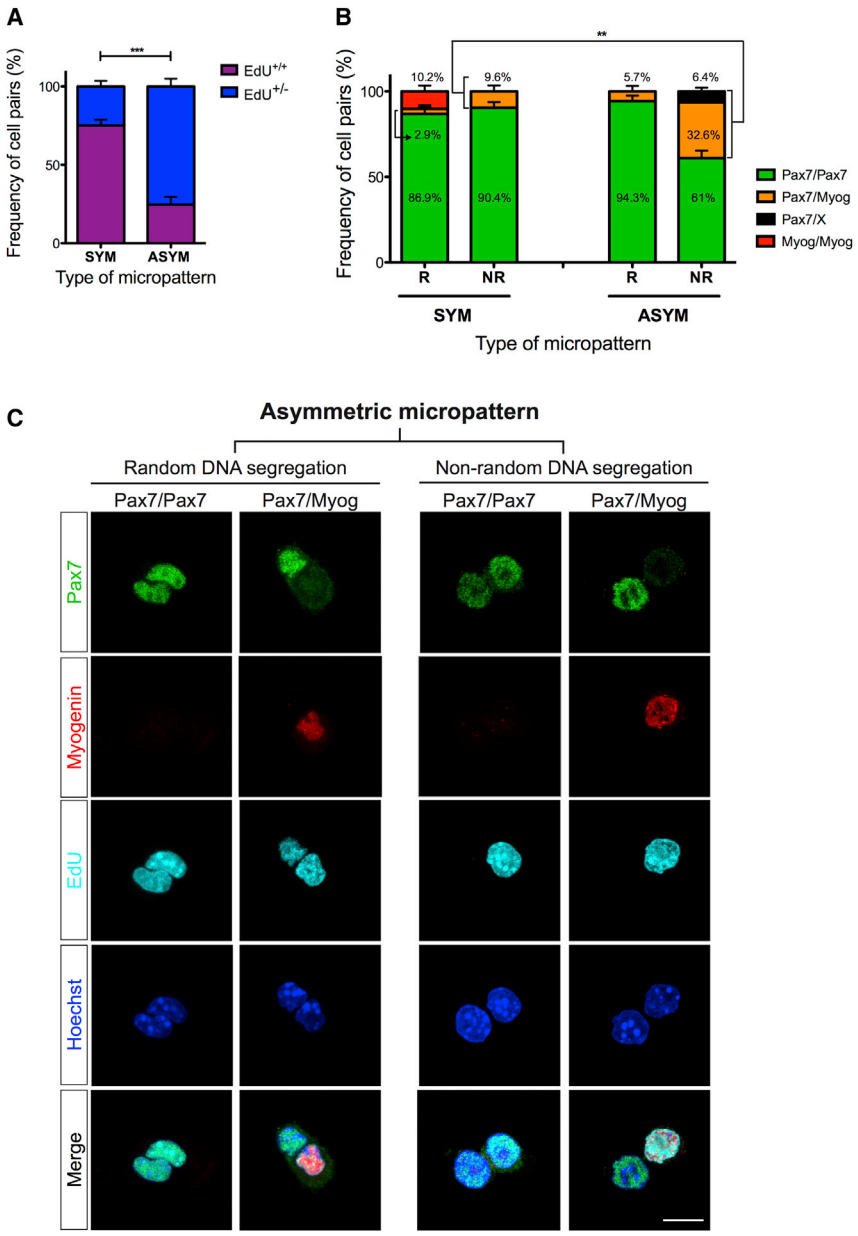

Figure 3. Cell Adhesion Topology Regulates Asymmetric Distribution of Transcription Factors and Correlates with Non-Random DNA Segregation

(A) Pax7-nGFP$^+$ myogenic cells were isolated by FACS from TA muscle of *Tg:Pax7-nGFP* mice as indicated in Figure 2D. Histogram shows the frequencies of DNA segregation patterns on symmetric and asymmetric micropatterns (n = 6 mice, obtained from those indicated in Figure 2E). Note that ASYM represents the average obtained from Asym1 and Asym2 motifs. Error bars indicated as SEM.

(B) Random and non-random DNA segregation patterns indicated in (A) were normalized in each category to 100%. Symmetric (Pax7/Pax7) and asymmetric (Pax7/Myogenin) transcription factor distributions were determined in cell pairs for each category on symmetric and asymmetric micropatterns. Note that Pax7/X cell pairs (X represents a Pax7-negative cell) were a minor fraction in which Pax7 stained only one daughter cell (data not shown). Error bars indicated as SEM.

(C) Examples of Click-iT chemical detection of EdU with anti-Pax7 and anti-Myogenin antibody immunostainings of daughter cell pairs indicated in (B) on the asymmetric micropattern. Examples of symmetric micropatterns are provided in Figure S2. Scale bar, 10 μm.

113 total cells, n = 6 mice; Figure 3A), and among these, the cell fates corresponded to 86.9% Pax7/Pax7, 2.9% Pax7/Myogenin, and 10.2% Myogenin/Myogenin. Further, 30% performed non-random DNA segregation (n = 35 of 113 total cells, n = 6 mice), with 90.4% Pax7/Pax7 and 9.6% Pax7/Myogenin where old DNA strands were retained in the Pax7$^+$ (EdU$^-$) cell (Figures 3A, 3B, and S2).

In contrast, the majority of the cells performed non-random DNA segregation on the asymmetric motifs (74%; n = 201 of 272 total cells, n = 6 mice; Asym1/Asym2 motifs combined), and among these, the cell fates corresponded to 61% Pax7/Pax7 and 32.6% Pax7/Myogenin or 6.4% Pax7/X (Figures 3A–3C). In the latter, a minor fraction of cells that were asymmetric for Pax7 but negative for Myogenin were noted, and these were scored as asymmetric fates. As with non-random DNA segregation on symmetric patterns, old DNA strands were retained in the Pax7$^+$ (EdU$^-$) cell. Random DNA segregation on asymmetric motifs corresponded to 26% of the total population (n = 71 of 272 total cells, n = 6 mice), with 94.3% Pax7/Pax7 and 5.7% Pax7/Myogenin (Figures 3A–3C and S2). Therefore, asymmetric cell fates were preferentially

(D) Scheme illustrating labeling of nascent DNA strands. To label nascent DNA strands ("exclusion" protocol), several pulses of nucleotide analog were administered for the equivalent of one cell division, resulting in labeled nascent strands in hemi-labeled DNA (Rocheteau et al., 2012). A second division during the chase is needed to distinguish labeled nascent DNA strands and unlabeled old template DNA strands in daughter cell pairs.

(E) Histogram showing the frequencies of non-random DNA segregation on one symmetric and two asymmetric micropattern motifs. Pax7-nGFP$^+$ myogenic cells were isolated from TA muscle of *Tg:Pax7-nGFP* mice as indicated in (D). Note that independent experiments were done with either EdU or BrdU from n = 9 mice ($p < 10^{-5}$). Data are represented as Label$^{+/+}$ or Label$^{+/-}$. Error bars indicated as SEM.

(F) Click-iT detection of EdU in examples of daughter cell pairs indicated in (E). The micropattern shapes are in red (schemes below).
Scale bars, 10 μm.

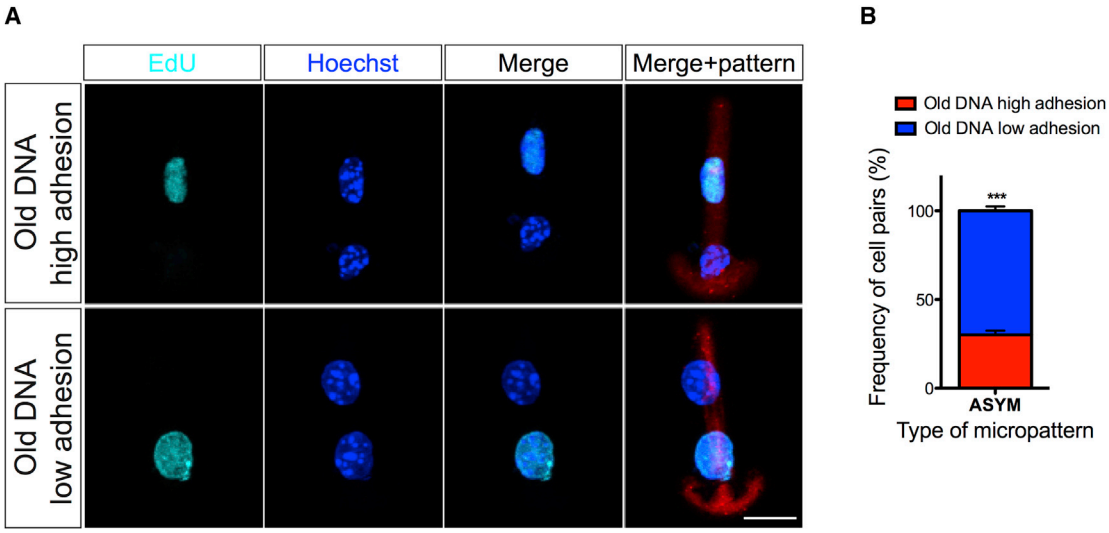

Figure 4. Old Template DNA Strands Are Associated with a Low-Adhesion Surface on Asymmetric Micropatterns

(A) Images of daughter cell pairs aligned along the asymmetric micropattern motif. Cells are labeled as indicated in Figure 2D.

(B) Histogram showing the frequencies of cells retaining old template DNA strands in association with high (curved side of micropattern) or low adhesion on asymmetric micropatterns. n = 168 cells, n = 3 mice; scale bar, 10 μm. Error bars indicated as SEM.

associated with non-random DNA segregation on both motifs, and cells that retained old DNA strands (EdU^-) were associated with Pax7 expression in Pax7/Pax7 and Pax7/Myogenin daughter cell pairs. In addition, 4-fold more asymmetric cell fates were associated with non-random DNA segregation on asymmetric motifs compared with symmetric motifs in this category (9.6% versus 39%). These observations also show that asymmetric cell fates tend to be associated with non-random DNA segregation; however, this correlation is not absolute, as these two events can be uncoupled.

Old Template DNA Strands Are Preferentially Associated with Low Adhesive Surface after Mitosis

The polarized microtubular network on asymmetric micropatterns, as well as the dominant effect of adhesion topology in determining asymmetric cell divisions outcomes, prompted us to assess whether old and new DNA strands show a bias relative to the extent of adhesion on the asymmetric micropattern motifs. To address this question, we examined EdU^+/EdU^- daughter cell pairs (see experimental protocol in Figure 2D) that were oriented along the long axis of the asymmetric micropattern motifs (Figure 4A). Interestingly, about 70% of cell pairs captured after mitosis had old template DNA strands (EdU^-) retained in the daughter cell that was located adjacent to the side with low adhesion (n = 51 of 168 total cell pairs, n = 3 mice; average of Asym1 and Asym2 motifs; $p < 0.0005$; Figure 4B).

Prospectively Isolated Cells Performing Non-Random DNA Segregation Resist Symmetric Micropattern Adhesion Cues

We showed previously that a subpopulation of muscle stem cells corresponding to the Pax7-nGFP^{Hi} fraction after isolation by FACS preferentially executed non-random DNA segregation (Rocheteau et al., 2012). Given the strong influence of extrinsic adhesion cues on determining the type of DNA segregation pattern, we asked whether manipulation of the spatial distribution of adhesion in micropatterns can override this decision in cells that are already engaged to perform non-random DNA segregation. Since relatively large numbers of cells are required for seeding on micropatterns, the top 20% of the total population corresponding to Pax7-nGFP^{Hi} cells was isolated by FACS (Figure 5A) and plated on nonpatterned fibronectin/fibrinogen Alexa Fluor 594-coated slides as a control. We noted that 68% of the cells performed non-random DNA segregation (Figures 5B and 5C; compared with 33% indicated above for the total population; Figure S1C), consistent with our previous findings that non-random DNA segregation is enriched in Pax7-nGFP^{Hi} muscle stem cells during regeneration.

When we examined the Pax7-nGFP^{Hi} population on the asymmetric motifs, we found that the majority of the cells performed non-random DNA segregation (75%; n = 146 of 194 total cells, n = 3 mice; Figures 5D and 5E; average of Asym1/Asym2 motifs), similar to the nonpatterned surface. Strikingly, when seeded on the symmetric motifs, the majority of the Pax7-nGFP^{Hi} cells continued to perform non-random DNA segregation (79%; n = 84 of 107 total cells, n = 3 mice; Figures 5D and 5E). Thus, prospectively isolated cells that perform non-random DNA segregation do not alter their mode of DNA distribution significantly when seeded on a symmetric micropattern.

DISCUSSION

Evidence for the asymmetric distribution of old and new DNA strands during cell division comes from studies in prokaryotes and eukaryotes (Yennek and Tajbakhsh, 2013). How this differential DNA strand identity can be registered during replication and then propagated to cells at the metaphase plate for selective distribution of chromatids containing old and new DNA strands is

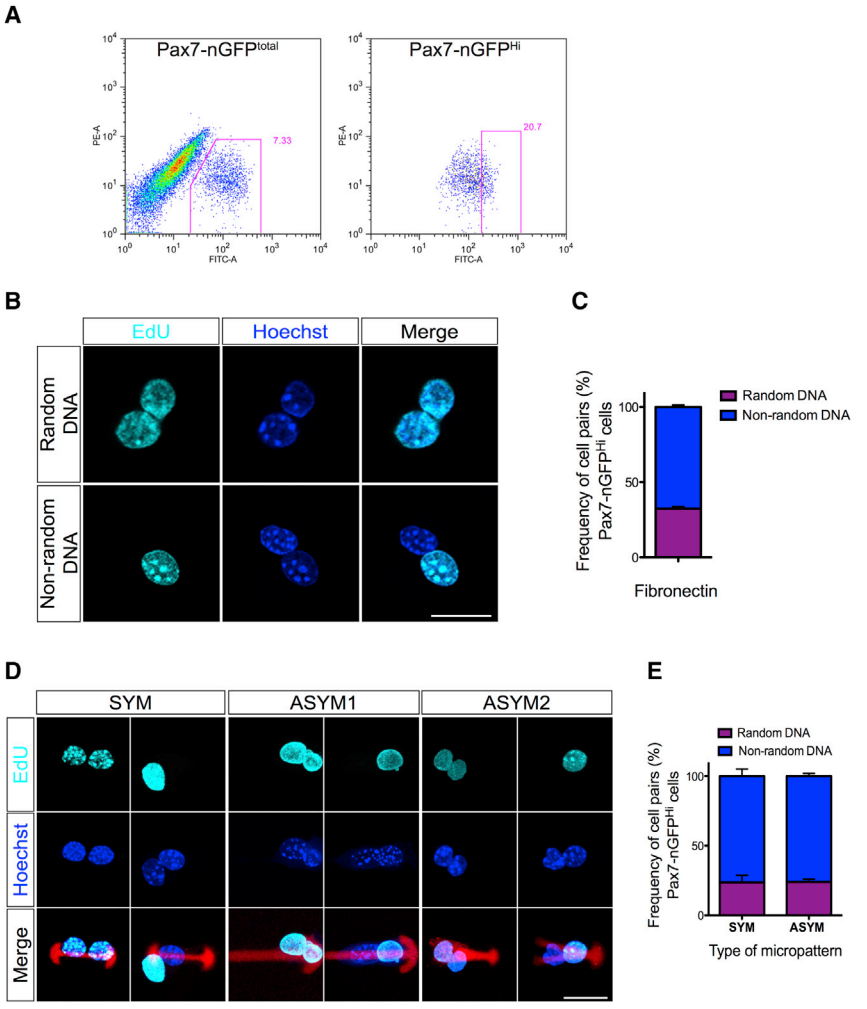

Figure 5. Prospectively Isolated Muscle Stem Cells Performing Non-Random DNA Segregation Resist Extrinsic Symmetry Adhesion Cues on Micropatterns

(A) FACS profiles of myogenic cells isolated from the TA muscle of *Tg:Pax7-nGFP* mice at 5 DPI. Total Pax7-nGFP and Pax7-nGFP^{Hi} (top 20%) cells are shown.

(B) Pax7-nGFP^{Hi} (top 20%) myogenic cells labeled with EdU (see Figure 2D) were isolated from TA muscles of *Tg:Pax7-nGFP* mice at 5 DPI and then plated on nonpatterned fibronectin/fibrinogen-Alexa Fluor 594-coated slides. Examples of random and non-random DNA segregation are shown. Cells were treated with 2 μM cytochalasin D for 2 hr to prevent cell separation.

(C) Histogram showing the frequencies of DNA segregation patterns as indicated in (B). Error bars indicated as SEM.

(D) Pax7-nGFP^{Hi} (top 20%) myogenic cells were isolated as indicated in (B) and seeded on symmetric and asymmetric micropatterns, and EdU staining was revealed by Click-iT chemistry. Micropatterns can be seen in red.

(E) Histogram showing the frequencies of DNA segregation patterns as indicated in (D). Note that ASYM represents the average obtained from Asym1 and Asym2 micropatterns (non-random DNA segregation: SYM, 84/107 cells; ASYM, 146/194 cells; n = 3 mice). Error bars indicated as SEM. Scale bar, 10 μm.

a major unresolved question. Although a clear mechanism to explain this phenomenon is still lacking for stem cells in vivo, studies have focused mainly on intrinsic factors that are largely epigenetic in nature (Elabd et al., 2013; Evano and Tajbakhsh, 2013; Lansdorp, 2007; Lew et al., 2008; Tajbakhsh and Gonzalez, 2009). A role for extrinsic cues in guiding template DNA segregation and cell fates has not been overtly explored. Here, we focused on extrinsic cell adhesion cues on micropatterned artificial niches. We report that by manipulating the spatial distribution of adhesion to the ECM, we could significantly alter the frequency of non-random DNA segregation and corresponding cell fates.

Various forms of mechanical stimuli, ECM, cell-cell contact, and signaling have been shown to play critical roles in the orientation of the plane of division to generate symmetric and asymmetric cell fates after mitosis (Chen et al., 2013; Engler et al., 2006; Freida et al., 2013). For the segregation of molecules associated with the membrane, cytoplasm, or nucleus, the axis of cell division, which is defined perpendicular to the spindle pole, is critical for asymmetric or symmetric outcomes. During mitosis, rotation of the spindle pole complex occurs before its final position is fixed, thereby determining the cell fate outcome (Li, 2013; Morin and Bellaïche, 2011). There is an additional level of complexity when DNA segregation patterns are considered. Old and new DNA strands are identified during DNA replication, and this information is thought to be retained in the condensed chromatin at metaphase prior to DNA segregation. As chromatids are aligned with the spindle pole apparatus, they will segregate to opposite poles along this axis. Therefore, extrinsic cues that can determine spindle pole orientation have been considered less likely (compared with intrinsic factors) to directly promote non-random DNA segregation (Lansdorp, 2007; Yennek and Tajbakhsh, 2013).

Several studies have shown that the behavior of individual or groups of cells and their differentiation on artificial surfaces can be modified on micropatterns (Blong et al., 2010; Freida et al., 2013; Gilbert et al., 2010; Li et al., 2011; Tang et al., 2010; Yu et al., 2013). For example, mesenchymal stem cells plated on microgrooves with regular patterns were reported to exhibit altered nuclear morphology, reduced levels of histone deacetylase activity, and increased histone acetylation (Li et al., 2011). Our finding that cell adhesion can regulate non-random DNA segregation patterns provides insights into the role of extrinsic cues in this process, and this finding is supported by a recent report that non-random DNA segregation in human bone marrow mesenchymal stem cells is regulated by cell adhesion differences on micropatterns (Freida et al., 2013). Interestingly, in that study, non-random DNA segregation patterns

involved some, but not all chromosomes as reported previously (Falconer et al., 2010; Yadlapalli and Yamashita, 2013), in contrast to muscle stem cells, where all chromatids are engaged in this process (Rocheteau et al., 2012). Furthermore, we obtained the highest frequencies reported for non-random DNA segregation in primary cells, and by manipulating cell adhesion were able to show that the majority of muscle stem cells are permissive for this type of asymmetric DNA segregation.

To understand the phenomenon of non-random DNA segregation, it is important to assess its relationship with the cell fates of the resulting daughter cells after cell division. We showed previously that asymmetric cell fates (stem, Pax7; differentiated, Myogenin) are associated with non-random DNA segregation in muscle stem cells on a population level (Rocheteau et al., 2012). Our present study of single cells dividing on micropatterns shows that both symmetric and asymmetric fates are associated with non-random DNA segregation. Interestingly, Pax7/Myogenin asymmetric fates were also found to be associated with random DNA segregation on micropatterns, and this frequency was higher on asymmetric micropatterns. Thus, cell adhesion cues play an important role in the regulation of both of these processes. Notably, non-random DNA segregation was not systematically correlated with the asymmetric distribution of Pax7 and Myogenin in resulting daughter cells. It is possible that we underestimated the overall frequency of asymmetric fates if the downregulation of Pax7 and concomitant upregulation of Myogenin take place well after mitosis has occurred. In this scenario, an intermediate asymmetric state would be scored as a symmetric Pax7/Pax7 event if the daughter cell pairs were captured immediately after mitosis. Our preliminary results suggest that this might be the case, since in Pax7/Pax7 daughter cell pairs, uneven Pax7 immunostainings were also observed in some cases, suggesting that one daughter cell might subsequently downregulate this marker. Nevertheless, our findings suggest that in some cases, DNA asymmetry and cell fate events can be uncoupled. We speculate that the frequency of non-random DNA segregation can be regulated by adhesion molecules located subjacent to the dividing stem cell in the niche in vivo. The coupling of this event with differential cell fates can occur, likely with the intervention of another event(s) that is as yet unidentified. In cases where non-random DNA segregation was associated with symmetric daughter cell fates, it is possible that the differential cells fates were not fixed; thus, subsequent rounds of asymmetric DNA distribution would need to be monitored. We note also that old template DNA strands were consistently inherited by the stem cell in Pax7/Myogenin daughter cell pairs independently of the labeling regime (labeling of old or new DNA with nucleotide analog) or the micropattern shape. Moreover, whether consecutive rounds of non-random DNA segregation occur without an intervening symmetric DNA distribution remains to be explored. Previous studies have reported that transcription factors can be distributed asymmetrically on isolated myofibers, as muscle stem cells divide planar and perpendicular to the myofiber and the basement membrane that ensheathes it (Cossu and Tajbakhsh, 2007; Kuang et al., 2007; Yennek and Tajbakhsh, 2013). Future studies with micropatterns can attempt to mimic this topology to explore the influence of different types of ECM on symmetric and asymmetric cell divisions.

Given that muscle stem cells are highly motile on micropatterns, continuously forming and releasing membrane contacts with the substrate in a dynamic manner (see Movies S1 and S2), we propose that the frequencies obtained for non-random DNA segregation and asymmetric cell fates were underestimated. In other words, a "symmetric" outcome can potentially arise on an asymmetric pattern depending on the probability of polarized contact with the substrate. Similarly, although symmetric patterns are designed to provide a homogeneous microenvironment, cells that release membrane contact on one side can experience temporary asymmetry with a certain probability, even on a symmetric micropattern. This can explain in part the finding that asymmetric outcomes were observed on symmetric micropatterns. Our findings lead us to propose that the adhesive geometry has a predominant effect on the fate of the dividing cells. With the caveat that extensive cell movements occur on the micropatterns, and in contrast to human bone marrow mesenchymal stem cells (Freida et al., 2013), the daughter cell that retained old template DNA strands was found to be preferentially associated with the low-adhesion side of the asymmetric micropattern motif following mitosis. We note, however, that extrinsic cues might be interpreted well before the initiation of mitosis. Future studies should focus on defining the timing of these events in relation to DNA segregation patterns and cell fates. It is also possible that other as yet undefined cues cooperate with cell adhesion to provide a second signaling event for guiding the type of cell division, as suggested above. Indeed, the nature of the substrate could potentially play a role, since fibronectin was suggested to modify Wnt signaling and increase symmetric cell division frequency (Bentzinger et al., 2013). A systematic evaluation of different ECM molecules, as well as the link among extrinsic cell adhesion cues, mother and daughter centrosomes, and kinetochore proteins (Evano and Tajbakhsh, 2013; Lansdorp, 2007; Lew et al., 2008; Tajbakhsh and Gonzalez, 2009) should be a major objective in future studies.

Finally, we report here that prospectively isolated muscle stem cells engaged in non-random DNA segregation resisted reversion to a random segregation pattern when seeded on symmetric micropatterns. Thus, our study shows that adhesion cues have a major impact on the type of DNA segregation pattern; however, this mechanism operates with a defined period corresponding to one cell cycle to regulate DNA segregation patterns. Beyond this window of opportunity, the non-random DNA segregation is irreversible. In summary, we provide evidence that the frequency of non-random DNA segregation and cell fates can be regulated by the spatial distribution of cell adhesion in skeletal muscle stem cells. The ability to control asymmetric and symmetric cell fates is of major interest for stem cell-based therapies in which a key objective is to maintain the stem cell state during amplification of the population ex vivo.

EXPERIMENTAL PROCEDURES

Micropatterns

After initial assessment of the size of activated myogenic cells was made, asymmetric (two types) and symmetric patterns were designed and manufactured on polystyrene-coated glass slides to allow spreading of single muscle stem cells or two daughter cells after cell division (Azioune et al., 2010). Due to the relatively small size of the myogenic cells, two asymmetric patterns

were designed, and they yielded similar results. Briefly, glass coverslips were spin coated at 3,000 rpm with a 1% solution of polystyrene in toluene. This polystyrene layer was further oxidized with an oxygen plasma treatment (Harrick Plasma) for 15 s at 30 W and incubated with poly-L-lysine polyethylene glycol (PLL-PEG; SuSoS) in 10 mM HEPES, pH 7.4, at room temperature (RT) for 30 min. PLL-PEG-coated slides were placed in contact with an optical mask containing transparent micropatterns (Toppan Photomask) using an in-house-made vacuum chamber and then exposed to deep UV light (Jelight). Micropatterned slides were subsequently incubated with a PBS solution containing 20 μg/ml fibronectin (Sigma) and 20 μg/ml Alexa Fluor 594-fibrinogen (Invitrogen) for 30 min and then rinsed three times in PBS. Coverslips were dried then rinsed in PBS before cell seeding.

Mice, Muscle Injury, and Injections of Thymidine Analogs

Animals were handled according to national and European community guidelines, and protocols were approved by an ethics committee. *Tg:Pax7-nGFP* mice were described previously (Sambasivan et al., 2009). Muscle injury was done as described previously (Gayraud-Morel et al., 2007). Briefly, mice were anesthetized with 0.5% Imalgene/2% Rompun. The Tibialis anterior (TA) muscle was injected with 10 μl of notexin (10 μM; Latoxan). 5-Bromo-2′-deoxyuridine (BrdU; #B5002; Sigma) and EdU (#E10187; Invitrogen) analogs were dissolved in 0.9% saline (GIBCO) and stored at 10 and 6 mg/ml, respectively. For the pulse-chase labeling after notexin injury, transgenic mice (6–10 weeks old) were injected intraperitoneally with 30 μg/g of EdU or 50 μg/g of BrdU. For the inclusion protocol, EdU was injected five times, 8 hr apart, from 3 DPI (Figure S1A). For the exclusion protocol, BrdU or EdU was injected three times, 2 hr apart, 14 hr prior to sacrifice (Figure S1A).

Muscle Stem Cell Isolation, Culture, and FACS

Dissections were done essentially as described previously (Gayraud-Morel et al., 2007). Injured TA muscles were removed from the bone in cold Dulbecco's modified Eagle's medium (DMEM; Invitrogen) containing 1% of penicillin-streptomycin (PS; Invitrogen), minced with scissors, and then digested with a mixture of 0.08% Collagenase D (Roche) and 0.2% Trypsin (Invitrogen) in DMEM/1% PS/DNase I (10 μg/ml; Roche) for five consecutive cycles of 30 min at 37°C. For each round, the supernatant was filtered through a 70 μm cell strainer and trypsin was blocked with 8% fetal calf serum (FCS; Invitrogen) on ice. Pooled supernatants from each digestion cycle were centrifuged twice at 1,600 rpm for 10 min at 4°C. Between centrifugations, pellets were resuspended in cold 2% FCS/1% PS/DMEM, washed with 1% PS/DMEM and filtered through a 40 μm cell strainer. Prior to FACS, the pellet was resuspended in 500 μl of cold 2% FCS/1% PS/DMEM and the cell suspension was filtered through a 40 μm cell strainer. Cells were sorted using a FACS Aria III (BD Biosciences) and collected in 1 ml of 2% FCS/1% PS/DMEM. Cells were displayed as phycoerythrin (PE, red) on the FACS profile. All analyses and quantitations were performed using FlowJo software. Satellite cells were cultured in 1:1 DMEM (Invitrogen)/MCDB (Sigma) containing 20% FCS, 2% Ultroser (Pall), and 1% PS. The medium was filtered through a 0.2 μm filter. Cells were cytospun on the chip at 40 *g* for 4 min, and 1 hr after plating, nonattached cells were washed with media. Cells were kept in an incubator (37°C, 5% CO_2, 3% O_2) for 12 hr.

Immunocytochemistry

For nuclear immunostainings, cells were fixed with 4% paraformaldehyde (PFA) in PBS 1× (GIBCO) and then washed three times with PBS 1×. Cells were permeabilized with 0.5% Triton X-100 5 min, washed once with PBS 1×, and blocked with 10% serum for 30 min. For the BrdU immunostaining, cells were unmasked with DNaseI (1,000 U/ml; Roche) for 30 min at 37°C prior to blocking. Cells were incubated with primary antibodies (Pax7, mouse monoclonal 1/30, DSHB; Myogenin, rabbit polyclonal, #sc-576, Santa Cruz, 1/200; anti-BrdU, BD, 1/100) for 3 hr at RT. Cells were washed with PBS 1× three times and incubated for 1 hr with Alexa-conjugated secondary antibodies (1/500; Life Technologies) and washed in PBS 1×. EdU staining was chemically revealed with the Click-iT kit (#C10640; Life Technologies). For cytoskeleton stainings, cells were fixed and permeabilized with 0.1% Triton X-100/0.5% glutaraldehyde in cytoskeleton buffer sucrose (CBS) for 10 min at RT and then washed three times with PBS 1×. Glutaraldehyde was reduced with 0.1 M glycine for 10 min at RT and then washed three times with PBS 1×. Cells were blocked in 3% BSA for 45 min at RT. Cells were incubated with anti-alpha-tubulin, rat monoclonal (#MCA77G, 1/1,000; Serotec) for 1 hr at RT. Cells were washed three times with PBS 1× and incubated with alexa 488-conjugated secondary antibody (1/500, Life Technologies) and phalloidin conjugated with rhodamine (1/1,000; Molecular Probes); stainings were protected from light. After three washes with PBS 1×, cells were incubated with Hoechst 33342 (1/1,000; stock 1 mg/ml). Chips were mounted with Slow Fade Gold reagent (#S3940; Life Technologies). Chips were analyzed with a Leica SPE confocal, Zeiss Observer Z1, and Zeiss LSM700. All antibodies were diluted in 0.1% BSA/0.1% Tween/PBS 1×. CBS contains 10 mM of 4-morpholineethanesulfonic acid (pH 6.1), 138 mM of potassium chloride, 3 mM of magnesium chloride, and 2 mM of ethylene glycol tetraacetic acid (Mitchison lab, Harvard Medical School; http://mitchison.med.harvard.edu/protocols.html).

Live Imaging

Cells isolated by FACS were plated on micropatterns as described above (Azioune et al., 2010). The plate was then incubated at 37°C, 5% CO_2, and 3% O_2 (Zeiss, Pecon). A Zeiss Observer.Z1 connected to an LCI PlnN 10×/0.8 W DICII objective and Hamamatsu Orca Flash 4 camera piloted with Zen (Zeiss) was used. Cells were filmed and images were taken every 8 min with bright-field and DICII filters (Zeiss). The raw data were transformed and presented as a video.

Statistics

Statistical analysis was performed with GraphPad Prism software using appropriate tests and a minimum of 95% confidence interval for significance (*$p < 0.05$, **$p < 0.001$, ***$p < 0.0001$). Graphs display the average values of all animals tested (SEM).

SUPPLEMENTAL INFORMATION

Supplemental Information includes two figures and two movies and can be found with this article online at http://dx.doi.org/10.1016/j.celrep.2014.04.016.

AUTHOR CONTRIBUTIONS

S.T., S.Y., and M.T. proposed the concept and designed the experiments. S.Y. performed the experiments. M.B. and M.T. designed and prepared the micropatterned chips. S.Y. and S.T. wrote the paper. All authors read and agreed with the manuscript.

ACKNOWLEDGMENTS

We thank Theo Cambier for the optical mask design and members of the lab for helpful discussions. S.T. acknowledges support from the Institut Pasteur, Agence Nationale de la Recherche (Laboratoire d'Excellence Revive, Investissement d'Avenir; ANR-10-LABX-73 and ANR-06-BLAN-0039), the Association pour la Recherche sur le Cancer, and the European Research Council (Advanced Research Grant 332893). S.Y. is funded by a PhD fellowship from La Ligue contre le Cancer. M.T. acknowledges support from the ERC (Starting Grant 310472) and the ISI program of BPIFrance.

Received: October 10, 2013
Revised: February 24, 2014
Accepted: April 9, 2014
Published: May 15, 2014

REFERENCES

Azioune, A., Carpi, N., Tseng, Q., Théry, M., and Piel, M. (2010). Protein micropatterns: a direct printing protocol using deep UVs. Methods Cell Biol. *97*, 133–146.

Bentzinger, C.F., Wang, Y.X., von Maltzahn, J., Soleimani, V.D., Yin, H., and Rudnicki, M.A. (2013). Fibronectin regulates Wnt7a signaling and satellite cell expansion. Cell Stem Cell *12*, 75–87.

Blong, C.C., Jeon, C.-J., Yeo, J.-Y., Ye, E.-A., Oh, J., Callahan, J.M., Law, W.D., Mallapragada, S.K., and Sakaguchi, D.S. (2010). Differentiation and behavior of human neural progenitors on micropatterned substrates and in the developing retina. J. Neurosci. Res. *88*, 1445–1456.

Cairns, J. (1975). Mutation selection and the natural history of cancer. Nature *255*, 197–200.

Chen, S., Lewallen, M., and Xie, T. (2013). Adhesion in the stem cell niche: biological roles and regulation. Development *140*, 255–265.

Conboy, M.J., Karasov, A.O., and Rando, T.A. (2007). High incidence of non-random template strand segregation and asymmetric fate determination in dividing stem cells and their progeny. PLoS Biol. *5*, e102.

Cossu, G., and Tajbakhsh, S. (2007). Oriented cell divisions and muscle satellite cell heterogeneity. Cell *129*, 859–861.

Elabd, C., Cousin, W., Chen, R.Y., Chooljian, M.S., Pham, J.T., Conboy, I.M., and Conboy, M.J. (2013). DNA methyltransferase-3-dependent nonrandom template segregation in differentiating embryonic stem cells. J. Cell Biol. *203*, 73–85.

Engler, A.J., Sen, S., Sweeney, H.L., and Discher, D.E. (2006). Matrix elasticity directs stem cell lineage specification. Cell *126*, 677–689.

Evano, B., and Tajbakhsh, S. (2013). Sorting DNA with asymmetry: a new player in gene regulation? Chromosome Res. *21*, 225–242.

Falconer, E., Chavez, E.A., Henderson, A., Poon, S.S., McKinney, S., Brown, L., Huntsman, D.G., and Lansdorp, P.M. (2010). Identification of sister chromatids by DNA template strand sequences. Nature *463*, 93–97.

Freida, D., Lecourt, S., Cras, A., Vanneaux, V., Letort, G., Gidrol, X., Guyon, L., Larghero, J., and Thery, M. (2013). Human bone marrow mesenchymal stem cells regulate biased DNA segregation in response to cell adhesion asymmetry. Cell Rep. *5*, 601–610.

Gayraud-Morel, B., Chrétien, F., Flamant, P., Gomès, D., Zammit, P.S., and Tajbakhsh, S. (2007). A role for the myogenic determination gene Myf5 in adult regenerative myogenesis. Dev. Biol. *312*, 13–28.

Gilbert, P.M., Havenstrite, K.L., Magnusson, K.E., Sacco, A., Leonardi, N.A., Kraft, P., Nguyen, N.K., Thrun, S., Lutolf, M.P., and Blau, H.M. (2010). Substrate elasticity regulates skeletal muscle stem cell self-renewal in culture. Science *329*, 1078–1081.

Huh, Y.H., and Sherley, J.L. (2011). Molecular cloaking of H2A.Z on mortal DNA chromosomes during nonrandom segregation. Stem Cells *29*, 1620–1627.

Karpowicz, P., Morshead, C., Kam, A., Jervis, E., Ramunas, J., Cheng, V., and van der Kooy, D. (2005). Support for the immortal strand hypothesis: neural stem cells partition DNA asymmetrically in vitro. J. Cell Biol. *170*, 721–732.

Kuang, S., Kuroda, K., Le Grand, F., and Rudnicki, M.A. (2007). Asymmetric self-renewal and commitment of satellite stem cells in muscle. Cell *129*, 999–1010.

Lansdorp, P.M. (2007). Immortal strands? Give me a break. Cell *129*, 1244–1247.

Le Grand, F., Jones, A.E., Seale, V., Scimè, A., and Rudnicki, M.A. (2009). Wnt7a activates the planar cell polarity pathway to drive the symmetric expansion of satellite stem cells. Cell Stem Cell *4*, 535–547.

Lew, D.J., Burke, D.J., and Dutta, A. (2008). The immortal strand hypothesis: how could it work? Cell *133*, 21–23.

Li, R. (2013). The art of choreographing asymmetric cell division. Dev. Cell *25*, 439–450.

Li, Y., Chu, J.S., Kurpinski, K., Li, X., Bautista, D.M., Yang, L., Sung, K.-L.P., and Li, S. (2011). Biophysical regulation of histone acetylation in mesenchymal stem cells. Biophys. J. *100*, 1902–1909.

Liu, W., Wen, Y., Bi, P., Lai, X., Liu, X.S., Liu, X., and Kuang, S. (2012). Hypoxia promotes satellite cell self-renewal and enhances the efficiency of myoblast transplantation. Development *139*, 2857–2865.

Minc, N., and Piel, M. (2012). Predicting division plane position and orientation. Trends Cell Biol. *22*, 193–200.

Morin, X., and Bellaïche, Y. (2011). Mitotic spindle orientation in asymmetric and symmetric cell divisions during animal development. Dev. Cell *21*, 102–119.

Neumüller, R.A., and Knoblich, J.A. (2009). Dividing cellular asymmetry: asymmetric cell division and its implications for stem cells and cancer. Genes Dev. *23*, 2675–2699.

Pine, S.R., Ryan, B.M., Varticovski, L., Robles, A.I., and Harris, C.C. (2010). Microenvironmental modulation of asymmetric cell division in human lung cancer cells. Proc. Natl. Acad. Sci. USA *107*, 2195–2200.

Potten, C.S., Owen, G., and Booth, D. (2002). Intestinal stem cells protect their genome by selective segregation of template DNA strands. J. Cell Sci. *115*, 2381–2388.

Quyn, A.J., Appleton, P.L., Carey, F.A., Steele, R.J., Barker, N., Clevers, H., Ridgway, R.A., Sansom, O.J., and Näthke, I.S. (2010). Spindle orientation bias in gut epithelial stem cell compartments is lost in precancerous tissue. Cell Stem Cell *6*, 175–181.

Rocheteau, P., Gayraud-Morel, B., Siegl-Cachedenier, I., Blasco, M.A., and Tajbakhsh, S. (2012). A subpopulation of adult skeletal muscle stem cells retains all template DNA strands after cell division. Cell *148*, 112–125.

Sambasivan, R., Gayraud-Morel, B., Dumas, G., Cimper, C., Paisant, S., Kelly, R.G., and Tajbakhsh, S. (2009). Distinct regulatory cascades govern extraocular and pharyngeal arch muscle progenitor cell fates. Dev. Cell *16*, 810–821.

Seale, P., Sabourin, L.A., Girgis-Gabardo, A., Mansouri, A., Gruss, P., and Rudnicki, M.A. (2000). Pax7 is required for the specification of myogenic satellite cells. Cell *102*, 777–786.

Shinin, V., Gayraud-Morel, B., Gomès, D., and Tajbakhsh, S. (2006). Asymmetric division and cosegregation of template DNA strands in adult muscle satellite cells. Nat. Cell Biol. *8*, 677–687.

Tajbakhsh, S., and Gonzalez, C. (2009). Biased segregation of DNA and centrosomes: moving together or drifting apart? Nat. Rev. Mol. Cell Biol. *10*, 804–810.

Tang, J., Peng, R., and Ding, J. (2010). The regulation of stem cell differentiation by cell-cell contact on micropatterned material surfaces. Biomaterials *31*, 2470–2476.

Théry, M., Racine, V., Pépin, A., Piel, M., Chen, Y., Sibarita, J.-B., and Bornens, M. (2005). The extracellular matrix guides the orientation of the cell division axis. Nat. Cell Biol. *7*, 947–953.

Théry, M., Jiménez-Dalmaroni, A., Racine, V., Bornens, M., and Jülicher, F. (2007). Experimental and theoretical study of mitotic spindle orientation. Nature *447*, 493–496.

Troy, A., Cadwallader, A.B., Fedorov, Y., Tyner, K., Tanaka, K.K., and Olwin, B.B. (2012). Coordination of satellite cell activation and self-renewal by Par-complex-dependent asymmetric activation of p38α/β MAPK. Cell Stem Cell *11*, 541–553.

Yadlapalli, S., and Yamashita, Y.M. (2013). Chromosome-specific nonrandom sister chromatid segregation during stem-cell division. Nature *498*, 251–254.

Yennek, S., and Tajbakhsh, S. (2013). DNA asymmetry and cell fate regulation in stem cells. Semin. Cell Dev. Biol. *24*, 627–642.

Yu, T., Chua, C.K., Tay, C.Y., Wen, F., Yu, H., Chan, J.K.Y., Chong, M.S.K., Leong, D.T., and Tan, L.P. (2013). A generic micropatterning platform to direct human mesenchymal stem cells from different origins towards myogenic differentiation. Macromol. Biosci. *13*, 799–807.